OXFORD UNIVERSITY PRESS | Radiation Protection Dosimetry

NATURAL RADIOACTIVITY OF THE CRYSTALLINE BASEMENT ROCKS OF THE PELORITANI MOUNTAINS (NORTH-EASTERN SICILY, ITALY): MEASUREMENTS AND RADIOLOGICAL HAZARD

Journal:	*Radiation Protection Dosimetry*
Manuscript ID	RPD-20-0285.R1
Manuscript Type:	Paper
Subject Index Term:	Radiation risks, Radon

NATURAL RADIOACTIVITY OF THE CRYSTALLINE BASEMENT ROCKS OF THE PELORITANI MOUNTAINS (NORTH-EASTERN SICILY, ITALY): MEASUREMENTS AND RADIOLOGICAL HAZARD

D. Romano[1,2*], F. Caridi[3], M. Di Bella[2], F. Italiano[2], S. Magazù[1], M. T. Caccamo[1], A. Tripodo[1], G. Faggio[4], R. Grillo[4], C. Triolo[5], G. Messina[4], A. Gattuso[2] and G. Sabatino[1]

[1] Dipartimento di Scienze Matematiche e Informatiche, Scienze Fisiche e Scienze della Terra (MIFT), Università di Messina, Messina 98166, Italy

[2] Istituto Nazionale di Geofisica e Vulcanologia, Palermo 90146, Italy

[3] Agenzia Regionale per la protezione dell'Ambiente della Calabria, Italy (ARPACal), Dipartimento di Reggio Calabria, Via Troncovito SNC, Reggio Calabria 89135, Italy

[4] Dipartimento di Ingegneria dell'Informazione, delle Infrastrutture e dell'Energia Sostenibile (DIIES), Università "Mediterranea", Reggio Calabria 89122, Italy

[5] Dipartimento di Ingegneria Civile, dell'Energia, dell'Ambiente e dei Materiali (DICEAM), Università "Mediterranea", Reggio Calabria 89122, Italy

[*] corresponding author: dromano@unime.it

Running Title: Natural radiation from NE Sicily rocks

Crystalline rocks can produce dangerous radiation levels on the basis of their content in radioisotopes. Here, we report radiological data from ten metamorphic and igneous rock samples collected from the crystalline basement of the Peloritani Mountains (Southern Italy). In order to evaluate the radiological properties of these rocks, the gamma radiation and the radon emanation have been measured. Moreover, since some of these rocks are employed as building materials, we assess the potential hazard for population connected to their use. Gamma spectroscopy was used to measure the ^{226}Ra, ^{232}Th and ^{40}K activity concentration whereas the radon emanation was investigated by using a RAD 7 detector. The results show ^{226}Ra, ^{232}Th and ^{40}K activity concentration values ranging from (17 ± 4) Bq kg^{-1} to (56 ± 8) Bq kg^{-1}, (14 ± 3) Bq kg^{-1} to (77 ± 14) Bq kg^{-1} and (167 ± 84) Bq kg^{-1} to (1760± 242) Bq kg^{-1} respectively. Values of the annual effective dose equivalent (*AEDE*) outdoor range from 0.035 to 0.152 mSv y^{-1} whereas the gamma index is in the range of 0.22 - 0.98. The ^{222}Rn emanation coefficient and the ^{222}Rn surface exhalation rate vary from (0.63 ± 0.3) % to (8.27 ± 1.6) % and from (0.12 ± 0.03) Bq m^{-2} h^{-1} to (2.75 ± 0.17) Bq m^{-2} h^{-1} respectively. The indoor radon derived from the building use of these rocks induces an approximate contribution to the annual effective dose ranging from 8 to 176 µSv y^{-1}. All the obtained results suggest that the crystalline rocks from the Peloritani Mountains are not harmful for the residential population, even though they induce annual effective doses due to terrestrial gamma radiation above the worldwide average values. Moreover, their use as building materials does not produce significant health hazards connected to the indoor radon exposure.

INTRODUCTION

All living organisms on Earth, including the world population, are constantly exposed to ionizing radiation coming from natural sources. Their effects to organs and tissues, if the radiation levels are very high, can produce serious consequences on health. Natural radiation results from terrestrial radionuclides occurring in the Earth's crust and mantle (e.g. ^{235}U, ^{238}U, ^{232}Th, ^{40}K and ^{87}Rb) and from cosmic rays coming from the outer space and from the Sun. Two components contribute to the exposure from natural radiation: i) the external exposure, caused by gamma radiation induced from terrestrial radionuclides and by cosmic radiation and cosmogenic radionuclides, and: ii) the internal exposure, related to inhalation and ingestion. According to UNSCEAR[1], the annual global average effective dose received by an individual due to natural radiation results to be 2.4 mSv.

Among all the radionuclides responsible for the natural radiation exposure, radon and its daughters (i.e. polonium and bismuth) are considered to provide the largest contribution[1]. Radon is an odorless inert noble gas and the main isotopes are: ^{222}Rn (half-life of 3.8 days), which occurs as intermediate product in the ^{238}U decay series and it is generated by the ^{226}Ra α decay; and ^{220}Rn (half-life of 55 s), that belongs to the decay serie for ^{232}Th and it is produced by the α decay of ^{224}Ra. A strong relationship between indoor radon exposure and the increase of the risk of lung cancer exists[2-6]. According to WHO[7], after tobacco smoking, radon is considered the second cause of lung cancer in the general population. Radon-related health hazards are connected to indoor radon deriving from soils and from building materials and to radon dissolved in domestic and drinking waters. Gamma rays from terrestrial radionuclides provide the second largest contribution to the annual effective dose[1]. Gamma radiation originates from ^{40}K and from radionuclides occurring in the ^{238}U and ^{232}Th series.

The Peloritani Mountains, characterized by the presence of crystalline rocks (granites and low to high-grade metamorphites), constitute the north-eastern portion of Sicily (Southern Apennines, Italy), an area interested by a complicated geodynamic setting where subduction, transtensive deformation and active extension processes coexist[8-14]. It is known that uranium and thorium occur in low to high concentrations in unmetamorphosed and metamorphosed felsic igneous rocks,

because during magmatic processes, these highly incompatible elements tend to accumulate in the residual Si-rich magma melt. Moreover, U and Th may also occur at high concentrations in meta-sediments, especially if rocks interact with metasomatic and/or hydrothermal fluids at low to medium temperatures. Consequently, metamorphic and felsic igneous rocks could represent dangerous radiation sources, and all the outcropping areas, such as the Peloritani Mountains, can be subjected to very high values of annual effective doses from natural radiation.

Taking into account these consideration, here we intend to assess the environmental impact and the radiological hazards for inhabitants, connected to the natural occurrence of the crystalline rocks of the Peloritani Mountains. Moreover, since these rocks are extensively used as building materials, the potential hazards due to their use in construction was also evaluated. To reach this aim, a multidisciplinary approach including gamma ray and alpha spectroscopy was used to constrain the radiological properties in terms of gamma radiation and radon emanation.

GEOLOGICAL SETTING

The Peloritani Mountains represent the southernmost portion of the Calabria-Peloritani Orogen (CPO) and constitute the north-eastern edge of Sicily (Figure 1). The CPO is composed of oceanic units and a series of continental units including a metamorphic basement and often, a Meso-Cenozoic sedimentary cover. The CPO is divided, from a physiographic point of view, in a northern sector including Catena Costiera and Sila Massif and a southern sector represented by Serre and Aspromonte Massifs in Calabria and Peloritani Mountains in Sicily[15]. In Sicily, the Peloritani Belt overthrusted the Alpine Tethys units (i.e. Sicilide Units of Ogniben[16]) deformed during the accretionary and collisional processes connected with the subduction and closure of the Alpine Tethys realm.

The Peloritani Mountains include different continental units forming a south-verging nappe system, which are characterized by distinct tectono-metamorphic portions divided into an upper and a lower complex[15]. The upper complex outcrops in the northern sector of the Peloritani Mountains (Figure 1) and is composed of the Aspromonte and the Mandanici metamorphic Units, which are separated by a regional thrust (the Aspromonte basal thrust[17]). The Aspromonte Unit represents the highest tectono-metamorphic unit of the Peloritani Belt and is mainly composed of Variscan fine-grained paragneiss and orthogneiss, with minor amphibolite gneisses and marbles. Late Variscan igneous rocks (~290 Ma[18]) intruded the high-grade metamorphic rocks of the Aspromonte Unit, generating dykes and small plutons (e.g. the stock of Capo Rasocolmo). The Mandanici Unit is composed of medium to low-grade metamorphic rocks such as phyllites with minor metamorphosed volcanic and

carbonate rocks, which were interested by a greenschist to lower amphibolite Variscan metamorphism.

The lower complex outcrops in the southern sector of the Peloritani Mountains (Figure 1), and it is made up by three similar tectonic Units (St. Marco d'Alunzio, Longi-Taormina Unit and Cape St. Andrea Units) including a Variscan crystalline basement overlaid by a Meso-Cenozoic sedimentary cover. The metamorphic rocks of the lower complex are composed of metamorphosed fine-grained sedimentary rocks (i.e. metapelites), sometimes interbedded by felsic porphyroids and meta-volcanic rocks with mafic to intermediate compositions[19-23].

The metamorphic and plutonic basement rocks are locally covered by Meso-Cenozoic sediments, unconformably overlaid by syn- to post-orogenic sedimentary sequences. The top of these sedimentary sequences consists of Pleistocene terrigenous deposits (called "Sabbie and ghiaie of Messina" formation) outcropping along the Tyrrhenian and the Ionian margins of the Peloritani Belt. They represent the remnant of old fluvial and deltaic systems generated in response to the uplift stage occurred in North-Eastern Sicily during the Quaternary[24]. They are composed of crystalline sands and gravels primarily deriving from erosion and dismantling of three different type of rocks: Late Variscan plutonites, orthogneisses and paragneisses, all belonging to the Aspromonte Unit.

MATERIALS AND METHODS

Samples

In this study, ten samples of crystalline rocks from the CPO basement outcropping in North-eastern Sicily were collected. Locations and coordinates of the sampled rocks are listed and plotted in Table 1 and Figure 1, respectively . The collected samples include rocks from:

1. the Aspromonte Unit (ASP1: Late Variscan monzogranite; ASP2: orthogneiss; ASP3: paragneiss; ASP4: amphibolite gneiss; ASP5: marble);
2. the Mandanici Unit (MAN1: phyllite);
3. the St. Marco d'Alunzio Unit (SMU1: metapelite);
4. the Longi-Taormina Unit (LTU1: metapelite; LTU2: felsic porphyroid; LTU3: intermediate meta-volcanite).

ASP2, ASP3 and ASP5 samples are currently mined and used in construction. ASP4, MAN1, SMU1, LTU1, LTU2 and LTU3 samples are not used as building materials, and therefore in this paper we examine the possible effects deriving from their potential use. Furthermore, ASP1, ASP2 and ASP3 compositions are representative of the "Sabbie and ghiaie of Messina" formation, which is extracted and used as inert material in bulk amounts (e.g. concrete).

182

183 **Sample preparation**

184 All samples were carefully cleaned in order to remove the macroscopic altered portions. Then, each
185 sample was crushed in an agate mill, and sieved in order to obtain a particle size less than 2 mm.
186 After that, in agreement with the procedure adopted in Lee et al.[25] and Sabatino et al.[26], samples
187 were dried in an oven for 24 h at a temperature of 105°C, and then cooled in a desiccator to constant
188 weight. Subsequently, samples were sealed in an airtight containers for more than four weeks; after
189 that, the secular equilibrium between ^{226}Ra and their daughters was attained and samples were ready
190 to be analysed for gamma ray spectroscopy at the laboratories of the ARPACal Reggio Calabria
191 Department and for the radon emanation at the laboratories of the MIFT Department of the Messina
192 University. The radon emanation was measured by means of a homemade airtight container
193 connected to a RAD 7 spectrometer in terms of: a) emanation coefficient (i.e. emanation fraction,
194 emanation factor), representing the number of radon atoms released from the solid matrix with
195 respect the number of radon atoms generated by radium decay[27]; b) exhalation rate, which is the
196 amount of radon released per unit time.

197

198 **Gamma spectroscopy**

199 Samples analyzed for the gamma spectrometry were packed in polyethylene plastic vial of 20 mL of
200 volume, in order to obtain a homogeneous geometry around the detector. The net weights of
201 samples were measured before the analysis.

202 Samples were counted for 70000 s and analysed to determine the ^{226}Ra, ^{232}Th and ^{40}K activity
203 concentration. The ^{226}Ra activity concentration was determined through the 295.21 keV and 351.92
204 keV ^{214}Pb and 1120.29 keV ^{214}Bi γ-lines, whereas the 911.21 keV and 968.97 keV ^{228}Ac γ-lines,
205 were used to calculate the ^{232}Th activity concentration. For ^{40}K, the evaluation was performed from
206 its γ-lines at 1460.8 keV. The setup was composed by two Ortec HPGe detectors and integrated
207 digital electronics. The first detector is a negative biased detector (GMX) with FWHM of 1.94 keV,
208 peak to Compton ratio of 65:1 and relative efficiency of 37.5 % at 1.33 MeV (^{60}Co). The second
209 one is a positive biased detector (GEM) with FWHM of 1.85 keV, peak to Compton ratio of 64:1
210 and relative efficiency of 40 % at 1.33 MeV (^{60}Co). Lead shields with copper and tin lining were
211 used to shield the detectors from environmental background. The efficiency and the energy
212 calibration were performed by using suitable standards. In particular, the Eckert and Zigler Nuclitec
213 GmgH traceable multinuclide radioactive standards (number AK 5901) were used; they cover the
214 energy range from 59.54 keV to 836 keV, and they were customized to clone the identical
215 geometries of samples in a water-equivalent epoxy resin matrix. Moreover, for the efficiency

transfer factors calculations with respect to the vial sample geometry, the ANGLE 4 code was employed (Angle4 Software Home Page[28]).

For data acquisition and analysis, the Gamma Vision (Ortec) software was used (see Caridi et al.[29] for further information). Key information such as energy, half-life, etc. about the investigated radionuclides, are contained in an appropriate library, which was used to identify them in the spectrum and then, to perform activity calculations and corrections.

The activity concentration of the investigated radioisotopes was calculated using the following formula:

$$C = \frac{N_E}{\varepsilon_E \gamma_d M t} \quad (1)$$

where N_E is the net area of the radioisotope photopeak, ε_E and γ_d indicate the efficiency and yield of the photopeak, M represents the mass of the sample (g) and t indicates the live time (s). The correction for the self-absorption effect was performed through the Gamma Vision software itself.

The measurement result uncertainty, coverage factor k=2, was determined considering the uncertainty of: i) the counting estimation; ii) the calibration source; iii) the efficiency calibration; iv) the background subtraction; v) the γ-branching ratio[29].

Outdoor radiological hazard due to gamma radiation: the absorbed dose rate and the annual effective dose equivalent (AEDE)

For the absorbed dose rate (D) determination, conversion coefficients were used as follows [1]:

$$D = 0.462 C_{Ra} + 0.604 C_{Th} + 0.0417 C_K \quad (2)$$

where C_{Ra}, C_{Th} and C_K are the activity concentrations (Bq kg^{-1}) of ^{226}Ra, ^{232}Th and ^{40}K in the analysed samples, respectively. The absorbed dose rate is expressed in nGy h^{-1}.

The annual effective dose equivalent outdoor received by an individual who stays over an area formed of the studied rocks ($AEDE_{outdoor}$, mSv y^{-1}), was estimated using the adsorbed dose rate by using a conversion factor of 0.7 Sv Gy^{-1} from adsorbed dose to effective dose, and an outdoor occupancy factor of 0.2[1]:

$$AEDE_{outdoor} = D \cdot 8760\ h \cdot 0.2 \cdot 0.7 \cdot 10^{-6} \quad (3)$$

Exposure to gamma radiation originating from building materials: the Gamma index

The exposure to gamma radiation originating from radionuclides in building materials was evaluated through the "gamma index", also known as "concentration index" [30, 31] (I):

$$I = \frac{C_{Ra}}{300\ \text{Bq kg}^{-1}} + \frac{C_{Th}}{200\ \text{Bq kg}^{-1}} + \frac{C_K}{3000\ \text{Bq kg}^{-1}} \quad (4)$$

where C_{Ra}, C_{Th} and C_K are the activity concentrations expressed in Bq kg^{-1} of ^{226}Ra, ^{232}Th and ^{40}K. The gamma index is generally used only as a screening tool for identifying materials that may induce a significant amount of gamma radiation[30].

Radon emanation measurements

The ^{222}Rn emanation coefficient was evaluated by enclosing 0.8 L of sample material in an airtight container whose volume is equal to 8 L, causing the growth of the radon activity concentration in the air volume. The experimental setup is similar to that reported in IAEA[32] and in Arabi et al.[33, 34]. The container was connected to a dryer unit filled with calcium sulphate ($CaSO_4$) and to an electronic radon detector (RAD 7, Durridge Co.) through a piping system forming a closed loop in which air circulates. Silicon sealing was installed along the piping system and along connections among the container and the pipes.

The RAD 7 Durridge was used to measure the radon activity concentration in the air volume. The RAD 7 detector (see the RAD 7 Manual[35]) is a solid-state ion-implanted planar silicon alpha detector, which is located inside an internal cell of 0.7 L. The measurement of radon activity concentrations is achieved by using the activity of relative daughters (i.e. polonium isotopes). The internal cell, having a hemispherical shape, is coated on the inside with an electrical conductor charged by a high voltage power circuit able to develop a potential of 2000/2500 V with respect to the alpha detector. Radon nuclei decaying within the internal cell produce transformed nuclei (i.e. polonium) as positively charged ions. The electric field inside the cell, allows to drive the positive charged particles straight onto the detector, which is arranged at the centre of the hemisphere. The short-lived polonium nuclei decay upon the detector's active surface, and the emitted alpha particles having a 50% probability of entering the detector. The electrical signal produced whenever an alpha particle enter the detector is proportional in strength to the energy of the alpha particle. Different isotopes have different alpha energies, and produce different strength signals. Concerning our experiment, the "Sniff" mode (see the RAD 7 Manual[35]) was adopted. With this setup, the RAD 7 Durridge uses only the ^{218}Po alpha peak to determine the ^{222}Rn concentration.

Samples were sealed in the airtight container for more than four weeks, in order to ensure the establishment of the secular equilibrium between ^{226}Ra and ^{222}Rn[32]. After that, the activity concentration of ^{222}Rn released from the sample into the air volume was measured by the RAD 7 by using a cycle of four hours in "Sniff" mode. Then, the ^{222}Rn emanation coefficient (ε) was determined by the following formula[32-34]:

$$\varepsilon = \frac{VC_{Rn}}{MC_{Ra}} \quad (5)$$

where C_{Rn} (Bq m^{-3}) is the measured radon activity concentration, C_{Ra} (Bq kg^{-1}) is the radium activity concentration, M (kg) is the mass of the sample and V (8.3× 10^{-3} m^3) is the effective volume of the system calculated by considering the volume of the container, of the sample, of the loop system and of the RAD 7 internal cell. Moreover, in order to avoid back diffusion effects, the effective volume of the system was >10 times larger than the pore volume of the samples[36, 37].

The radon activity concentration in the container increases exponentially and tends to an equilibrium value. Knowing the equilibrium value, which corresponds to C_{Rn} (i.e. the activity concentration of ^{222}Rn measured by the RAD 7 detector), it is possible to calculate the ^{222}Rn exhalation rate, as follows[32, 38]:

$$E = \frac{C_{Rn}(\lambda + \lambda l)V}{X} \quad (6)$$

where λ (7.56 × 10^{-3} h^{-1}) is the radon decay constant, λl is the container leakage rate (6.96 × 10^{-3} h^{-1}), V (8.3× 10^{-3} m^3) is the effective volume of the system and X is the sample's surface area (m^2) or the mass of the sample (kg) depending on whether the exhalation rate is expressed as surface exhalation rate (E_S, Bq m^{-2} h^{-1}) or mass exhalation rate (E_M, Bq kg^{-1} h^{-1}), respectively.

The leakage from container (λl) was determined by continuously measuring the ^{222}Rn concentration exhaled from one of the samples (i.e. the Mandanici phyllite) in the container at interval of 2 hours for 6 days. The series of the measured ^{222}Rn concentrations were fitted to the equation expressing the radon activity growth as a function of time[38]:

$$C_t = C_0 e^{-t(\lambda + \lambda l)} + C_e(1 - e^{-t(\lambda + \lambda l)}) \quad (7)$$

where C_t is the ^{222}Rn concentration at time t, C_0 and C_e are the ^{222}Rn concentration at t=0 and at equilibrium, respectively, and λ is the radon decay constant. The experimental data fitted well with the model described, and λl of the experimental setup was obtained.

Calculation of indoor radon concentration and indoor effective dose

The indoor radon concentration depends on various factors, such as radon coming from soil beneath buildings and radon exhaled from building materials. It is possible to estimate the contribute to the indoor radon activity concentration in a room ($Ci_{Rn(bm)}$, Bq m^{-3}), originating from radon exhalation from building materials, knowing their surface exhalation rates by the following equation[38-40]:

$$Ci_{Rn(bm)} = \left[\sum_{i=1}^{n} w_{si} \cdot E_{Si}\right] \frac{S}{V\lambda_v} \quad (8)$$

where E_{si} (Bqm^{-2}h^{-1}) is the surface exhalation rate of the building material, w_{si} is the fractional usage of the building material, S/V (m^{-1}) is the surface to volume ratio of the room and λ_v (h^{-1}) is the annual average ventilation rate.

In addition, the annual effective dose induced by indoor radon exhaled from building materials (H, μSv y^{-1}) can be calculated using an indoor occupancy factor of 0.8, a ^{222}Rn equilibrium factor of 0.4, and a dose conversion factor for ^{222}Rn of 9 nSv (Bq h m^{-3})$^{-1}$ as follows[1]:

$$H = Ci_{Rn(bm)} \cdot 8760\ h \cdot 0.8 \cdot 0.4 \cdot 9 \cdot 10^{-3} \quad (9)$$

RESULTS AND DISCUSSION

^{226}Ra, ^{232}Th and ^{40}K occurring in the Peloritani rocks and soils generate a natural gamma radiation that produce exposures to humans. The activity concentrations of these terrestrial radionuclides were measured and adopted to compute the absorbed dose rate and the annual effective dose equivalent outdoor. Moreover, to test if the use in building construction might be of concern, the gamma index (I) was calculated.

The radon emanation from rock samples was investigated by calculating the ^{222}Rn emanation coefficient and the ^{222}Rn surface and mass exhalation rate. The ^{222}Rnsurface exhalation rate was used to perform a rough preliminary estimation of the contribution to the radon indoor, of radon originating from the use of the Peloritani crystalline rocks as building materials as well as the effective doses induced to residents.

Outdoor gamma radiation

The values of activity concentrations of ^{226}Ra, ^{232}Th and ^{40}K in the investigated samples are reported in Table 2. Experimental results range from (17 ± 4) Bq kg^{-1} to (56 ± 8) Bq kg^{-1}, from (14 ± 3) Bq kg^{-1} to (77 ± 14) Bq kg^{-1} and from (167 ± 84) Bq kg^{-1} to (1760 ± 242) Bq kg^{-1} for ^{226}Ra, ^{232}Th and ^{40}K, respectively.

LTU2 and LTU3 samples show the highest activity concentrations of respectively ^{226}Ra (56 ± 8 Bq kg^{-1}) and ^{40}K (1760 ± 242 Bq kg^{-1}), whereas the highest specific activity of ^{232}Th was detected in ASP2, ASP3, MAN1 and LTU3 samples, which exhibit values higher than 60 Bq kg^{-1}.

On the other hand, the ASP5 sample displays the lowest experimental values for ^{226}Ra (17 ± 4 Bq kg^{-1}) and ^{232}Th (14 ± 3 Bq kg^{-1}), while the ASP4 sample exhibits the lowest ^{40}K value (167 ± 84 Bq kg^{-1}).

The activity concentrations of ^{226}Ra, ^{232}Th and ^{40}K in the crystalline basement of the Peloritani Belt were compared with literature data of other European Countries and with the average worldwide values (UNSCEAR[1] and references therein). The comparison, shown in Figure 2, highlights that

the Peloritani rocks exhibit values of ^{40}K activity concentration higher than those of both European Countries and worldwide average, whereas ^{226}Ra and ^{232}Th specific activities result to be quite similar.

The adsorbed dose rate (D) and the corresponding annual effective dose equivalent outdoor ($AEDE_{outdoor}$) were calculated to estimate the radiological hazard effect due to terrestrial gamma rays emitted from the analysed rocks. The results are reported in Table 2. The adsorbed dose rates induced by the crystalline rocks are in the range of 28 - 123 nGy h^{-1}.

ASP2 and LTU2 samples show the highest $AEDE_{outdoor}$ value: 0.152 mSv y^{-1}. Values above 0.1 mSv y^{-1}, were calculated for ASP3, MAN1 and LTU3 samples. Conversely, the lowest values are those of ASP4 and ASP5 samples, 0.035 mSv $y^{-1}$and 0.074 mSv y^{-1} respectively.

All values except that for the ASP4 sample are higher than the worldwide average value of 0.07 mSv y^{-1}[1]. Despite this evidence, according to the Italian legislation[41] these values are not hazardous for inhabitants who spend their lives over areas characterized by the presence of the crystalline rocks studied in this paper.

However, those values should be referred to and individual who stays over the studied rocks. If soil is present above the bedrock, the dose rate will be presumably lower than that for a rock with the same natural activity concentration of ^{226}Ra, ^{232}Th and ^{40}K, since soils are less dense than rocks and usually they contain a percentage of moisture.

Gamma Index

The gamma index (I) was calculated with the aim of evaluating the hazard connected to the exposure to gamma rays emitted from the crystalline rocks when they are used in construction. The gamma index acts as a screening tool in identifying materials that could produce an increase to the annual effective dose higher than 1 mSv. According to EC[31], dose increases of 1 mSv y^{-1} are reached with I values of 1 if the material is used in bulk amounts, and with I values 6 if the material is used as tiles, boards or other restricted uses. Building materials should be exempted from restrictions when their gamma radiation increases the annual effective doses up to 1 mSv y^{-1}, as referred in Article 75 reported in Euratom Directive [30].

All the analysed samples display I values $\leq$ 1 (Table 2); therefore, the building use is allowed. However, ASP2, ASP3, MAN1, LTU2 and LTU3 samples show gamma index values between 0.76 and 0.98, which are slightly below the reference limit. Then, controls and additional measurements for these lithologies are suggested.

Concerning the “Sabbie and ghiaie of Messina”, which are broadly used in bulk amounts (as inert in concrete), the mineralogical content of these deposits abruptly varies from an area to another one in

relationship with the prevailing lithology from which the sediments were locally eroded. For this reason, and since radiological and mineralogical properties of sediments reflect those of the eroded parent rocks, we decided not to collect a sample of "Sabbie and ghiaie of Messina", but to analyse only their parent rocks (ASP1, ASP2 and ASP3 samples). Since the parent rock samples show *I* values in the range of 0.62 - 0.98, we can assume that additional measurements are required for safety use of the "Sabbie and ghiaie of Messina".

Natural radioactivity due to radon

The ^{222}Rn emanation coefficients (ε) of the studied samples, calculated through the activity concentration of ^{222}Rn released into the air volume of the sealed container, are reported in Table 3. The emanation coefficient depends on various factors: radium distribution, grain size, grain shape, temperature, moisture, specific surface and mineralogy[27, 32, 42, 43]. Also alteration and weathering processes can affect the emanation coefficient value[44, 45]. The ^{222}Rn emanation coefficient of the studied samples vary from (0.63 ± 0.3) % to (8.27 ± 1.6) % (Table 3). These values are comparable with representative literature data reporting emanation coefficients from soils and rocks in the range of 0.1 - 40 % (Sakoda et al.[27] and references therein). Since experimental conditions (i.e. temperature, moisture, radium distribution, grain size and shape) are similar for all samples, the only factors responsible for the different values of emanation coefficient among the crystalline rocks are the mineralogical content and the alteration degree.

The Late Variscan monzogranite (ASP1 sample) shows an emanation coefficient value of (2.44 ± 0.9) %, which is comparable with values of unaltered granites (around 1 - 2 %[34, 45]) since weathered and altered granites can reach values higher than 20 %[45].

A wide record of data is reported in the literature for gneisses[34, 46], which commonly exhibit ε values varying from 1 to 14%. The results of this study fit well in that range, as orthogneiss (ASP2 sample) and paragneiss (ASP3 sample) display emanation coefficients of (8.27 ± 1.6) % and (2.30 ± 0.7) %, respectively.

The ε values of (5.81 ± 1.3) % measured for the phyllite of the Mandanic Unit (MAN1 sample) is quite similar to literature data for phyllitic metamorphic rocks (7.7 %[25]).

The Aspromonte marble (ASP5 sample) was collected at Cape Tindari, where the active tectonic lineaments of the Tindari Fault System allow the upward rise of mantle and crustal fluids which can easily alter the hosting rocks[47]. The authors detected an intense rotten-eggs smell, which is a typical feature of sulfurous gases and minerals, during sampling activities and during rock crushing in laboratory. It could be an evidence that marbles suffered a low degree secondary alteration; although no secondary minerals (e.g. sulfur-bearing minerals) were detected in the XRPD pattern.

Therefore, the secondary alteration processes supposedly affecting marbles might have modified the pristine radon emanation power of the ASP5 sample as weathering and alteration usually increase the emanation coefficient of rocks[44, 45]. Nevertheless, the ASP5 sample exhibits a ^{222}Rn emanation coefficient of (5.99 ± 1.9) %, which lies inside the range for carbonate rocks provided by previous studied (limestones: 1.6 - 2.2 % and 6.8 - 13.2 %; Barretto[46] and Lee et al.[25], respectively; marbles: 8.5 % and 9.54 - 16.42 %; El Afifi et al.[48] and Misdaq and Amghar[49], respectively).

The radon emanation coefficients calculated in this work can be used to estimate the theoretical ^{222}Rn activity concentration (i.e. the chemical ^{222}Rn background concentration) in soils formed from the crystalline rocks studied here[50]. Soil radon values higher than the chemical background, generally highlight the presence of radon anomalies related to the occurrence of fault zones allowing the upward migration of deep gases (e.g. CO_2, CH_4, He and Rn).

Table 3 summarizes the ^{222}Rn surface (E_S) and mass (E_M) exhalation rates calculated for each samples. E_S and E_M values were derived to be in the range of (0.12 ± 0.03) Bq m^{-2} h^{-1} - (2.75 ± 0.17) Bq m^{-2} h^{-1} and (2.47 ± 0.69) mBq kg^{-1} h^{-1} - (54.02 ± 3.26) mBq kg^{-1} h^{-1} respectively.

The highest ^{222}Rn surface exhalation rates (2.75 ± 0.17 Bq m^{-2} h^{-1} and 1.56 ± 0.12 Bq m^{-2} h^{-1}) were measured for the orthogneiss (ASP2 sample) and the phyllite (MAN1 sample), respectively. These values have been compared with those of a number of natural materials often used in construction in Italy. The ^{222}Rn surface exhalation rates of orthogneisses and phyllites from Peloritani Mountains are similar to those of several volcanic products from the Roman comagmatic province (Central Italy) such as the "Tufo Lionato" from Colli Albani district (0.86 - 1.40 Bq m^{-2} h^{-1}; Tuccimei et al.[37]), the "Peperino" from Colli Albani districts (1.33 - 3.42 Bq m^{-2} h^{-1}; Tuccimei et al.[37], the "Lava" from Nemi (2.23 - 2.48 Bq m^{-2} h^{-1}; Tuccimei et al.[37]), and the "Lapilli" from Colli Albani districts (2.41 - 4.01 Bq m^{-2} h^{-1}; Tuccimei et al.[37]). However, orthogneiss and phyllite surface exhalation rates are much lower than those of building materials characterized by a high attitude to release radon (e.g. "Black pozzolana" from Colli Albani district 37 Bq m^{-2} h^{-1}, "Tufo rosso" from Vico district 5.47 - 17.06 Bq m^{-2} h^{-1} and "Tufo giallo napoletano" from Campania Region 2.66 - 10.33 Bq m^{-2} h^{-1}; Tuccimei et al.[37]); then, we should not considered them as a severe menace to the public health.

Concerning the Aspromonte marble (ASP5 sample), it display a ^{222}Rn surface exhalation rate of (0.82 ± 0.09) Bq m^{-2} h^{-1}, which is higher than those of the most famous carbonate rocks used as building materials in Italy (e.g. "Rosso Veronese" from Veneto Region 0.04 Bq m^{-2} h^{-1}, and "Travertino" from Tivoli 0.05 - 0.065 Bq m^{-2} h^{-1}; Tuccimei et al.[37]). However, marble samples analysed in other studies showed surface exhalation rates rather similar to that calculated for the ASP5 sample (e.g. 0.74 Bq m^{-2} h^{-1}; Kumar et al.[51]).

The E_S value of 0.30 ± 0.05 Bq m^{-2} h^{-1} measured for the Late Variscan monzogranite (ASP1 sample) is in agreement with the radon exhalation data coming from coeval granitoid rocks intruding the continental crust of Sardinia (0.11 to 0.91 Bq m^{-2} h-1; Dentoni et al.[38]). Late Variscan plutonites of Peloritani Mountains and Sardinia also show analogous ^{226}Ra activity concentrations (18 ± 4 Bq kg^{-1} of the ASP1 sample vs 18 to 80 Bq kg^{-1} of the Sardinian rocks[38]). For these reasons, as already suggested by Dentoni et al.[38], we carefully believe that the intrusive rocks generated within the European continental crust of Sardinia, Sicily and Calabria during the latest phase of the Variscan Orogeny (hence they formed in the same geodynamic setting), are characterized by similar radiological features.

Radium content exhibits a very poor correlation when plotted against radon emanation coefficient, surface exhalation rate and mass exhalation rate (not shown). Several studies[38, 52, 53] highlighted a similar behaviour testifying that radon emission from rocks mainly depends on mineralogical and physical characteristics of the solid matrix.

Hazard from radon in indoor settings

The indoor radon in dwellings, schools and workplaces mainly originates from soil gas infiltration. The reference level to minimize health hazards due to indoor radon exposure is 300 Bq m^{-3} (WHO[7]). Radon emanation from building materials is the second major source to indoor radon, and considering a model building in a temperate climate, its contribution to the indoor radon activity concentration is around 20 %[54].

As a result, determining the radon emanation from building materials might be very helpful to estimate health risks connected with the indoor radon exposure. For this purpose, we performed a preliminary evaluation of the contribution to the indoor radon deriving from the use of the Peloritani crystalline rocks in construction.

The indoor radon concentration coming only from radon emanation from building materials ($Ci_{Rn(bm)}$) was calculated by equation 8 by using the estimated surface exhalation rates for the crystalline rocks, a surface/volume ratio S/V = 1.6 m^{-1} considering a room model with dimensions of (4 x 5 x 2.8) m^3 and a ventilation rate λ_v = 0.63 h^{-1} (UNSCEAR[1]). Moreover, equation 9 assesses the human exposure to indoor radon through calculation of annual effective doses (H). The calculated $Ci_{Rn(bm)}$ and H values are reported in Table 3.

The orthogneiss (ASP2 sample) shows a $Ci_{Rn(bm)}$ of 6.99 Bq m^{-3} that corresponds to an effective dose of 176 µSv per year. These values are the highest among the collected samples.

The phyllite (MAN1 sample) and the felsic porphyroid (LTU2 sample) exhibit indoor radon activity concentrations higher than 3 Bq m^{-3} and effective doses induced to humans of 100 µSv y^{-1} and 81 µSv y^{-1}, respectively. In contrast, other samples show H values lower than 60 µSv y^{-1}.

Considering the indoor radon reference limit of 300 Bq m^{-3} and a 20 % contribution from building materials, the analysed rocks should produce $Ci_{Rn(bm)}$ values not exceeding 60 Bq m^{-3} in order to minimize health hazards. All the crystalline rocks studied in this paper show $Ci_{Rn(bm)}$ values well below the 60 Bq m^{-3} threshold (Table 3); therefore, their use as building materials does not produce significant health risks due to indoor radon exposure. Also the use of the "Sabbie and ghiaie of Messina" formation seems to be not hazardous as their parent rocks (paragneisses, monzogranites and orthogneisses) exhale radon at low rates.

The indoor radon concentrations originating from the use of the studied materials, and the corresponding annual effective doses received by humans, represent only rough estimations as some limitations have to be taken into account: i) in the calculation we considered walls, the ceiling and the floor exclusively composed of the analysed material (surface fractional usage w_{si}= 100%); ii) the "Sabbie and ghiaie of Messina" formation is largely used in construction, but collecting a representative sample was not possible due to the huge vertical and lateral variability of the mineralogical content within this formation; for this reason we analysed only their parent rocks (paragneisses, orthogneisses and monzogranites); iii) we assumed walls, the ceiling and the floor made up by the studied sample in the same form as during the experiment, namely in granular form; but we have to consider that both radon diffusion length and radon surface exhalation rate, on which the indoor radon concentration depends, can vary according to material shape and fabric.

Therefore, the calculated $Ci_{Rn(bm)}$ and H values should be attributed only to extreme situations, adopted to preliminarily assess the radon potential risk associated with the use in construction of the crystalline rocks from Peloritani Mountains.

CONCLUDING REMARKS

This study demonstrates that the crystalline rocks outcropping in the Peloritani Mountains do not induce hazardous annual effective doses due to gamma rays emitted by terrestrial radionuclides (^{226}Ra, ^{232}Th and ^{40}K). Moreover, their usage as building materials is not harmful in terms of radon exposure. In fact, these rocks seem not to produce a contribution to the indoor radon concentrations that are able to cause the exceeding of the recommended reference limit of 300 Bq m^{-3}, representing the maximum acceptable level to minimize health hazards.

Nevertheless, since North-eastern Sicily is affected by an intense seismic activity[55], and the relationship between tectonic activity and anomalous emission of gases including radon was widely

demonstrated by several scientific studies[56-61], we cannot completely ruled out the possibility that along fault zones the upward migration of deep fluids produces high natural radiation levels due to radon.

Radon released from soils can easily enter buildings from floor and walls cracks and discontinuities; underground spaces and rooms located at ground floor are the most vulnerable places. For this reason, we believe that further radiological analyses should be performed in order to better constraint if there are specific areas where the resident population is exposed to dangerous radiation doses. For instance, a series of surveys involving the measurements of soil radon concentration along tectonic lineaments and the evaluation of indoor radon levels in houses, schools and public edifices could be useful.

ACKNOWLEDGMENTS

The authors wish to thank the FSE (Fondo Sociale Europeo) operational program (OP) for Sicily 2014-2020 for its financial support. Moreover, we thank two anonymous referees who greatly improved the quality of the manuscript.

REFERENCES

(1) UNSCEAR. *Report to general assembly of the United Nations Scientific Committee on the effects of atomic radiation.* United Nations New York (2000).

(2) Lubin, J. H. ,Wang, Z. Y., Boice Jr, J. D., Xu, Z. Y., Blot, W. J., De Wang, L. and Kleinerman, R.A. *Risk of lung cancer and residential radon in China: pooled results of two studies*. Int. J. Cancer **109,** 132-7 (2004).

(3) Darby, S., Hill, D., Auvinen, A., Barros-Dios, J. M., Baysson, H., Bochicchio, F., Deo, H., Falk, R., Forastiere, F., Hakama, M., Heid, I., Kreienbrock, L., Kreuzer, M., Lagarde, F., Makelainen, J., Muirhead, C., Oberaigner, W., Pershagen, G., Ruano-Ravina, A., Ruosteenoja, E., Rosario, A. S., Tirmache, M., Tomasek, L., Whitley, F., Wichmann, H. E., and Doll, R. *Radon in homes and risk of lung cancer: collaborative analysis of individual data from 13 European case-control studies*. Br. Med. J. **330**, 223-226 (2005).

(4) Darby, S., Hill, D., Deo, H., Auvinen, A., Barros-Dios, J. M., Baysson, H., Bochicchio, F., Falk, R., Farchi, S., Figueiras, A., Hakama, M., Heid, I., Hunter, I., Kreienbrock, L., Kreuzer, M., Lagarde, F., Makelainen, J., Muirhead, C., Oberaigner, W., Pershagen, G., Ruosteenoja, E., Rosario, A. S., Tirmache, M., Tomasek, L., Whitley, F., Wichmann, H. E., and Doll, R. *Residential radon and lung cancer--detailed results of a collaborative analysis of individual data on 7148 persons with lung cancer and 14,208 persons without lung cancer from 13 epidemiologic studies in Europe*. Scand. J. Work, Env. Hea. **32,**1-83 (2006).

(5) Krewski, D., Lubin, J. H., Zielinski, J. M., Alavanja, M., Catalan, V. S., Field, R.W., Klotz, J. B., Letourneau, E. G., Lynch, C. F., Lyon, J. L., Sandler, D. P., Schoenberg, J. B., Steck, D. J., Stolwijk, J. A., Weinber, C. and Wilcox, H. B. *Residential radon and risk of lung cancer: a combined analysis of 7 North American case-control studies*. Epidemiology **16**, 137-145 (2005).

(6) Krewski, D., Lubin, J. H., Zielinski, J. M., Alavanja, M., Catalan, V. S., Field, R.W., Klotz, J. B., Letourneau, E. G., Lynch, C. F., Lyon, J. L., Sandler, D. P., Schoenberg, J. B., Steck, D. J., Stolwijk ,J. A., Weinber, C. and Wilcox, H. B. *A combined analysis of North American case-control studies of residential radon and lung cancer*. J. Toxicol. Environ. Health A. **69**, 533-597 (2006).

(7) WHO. *Handbook on indoor Radon: a public health perspective.* World Health Organization Geneva (2009).

(8) Monaco, C. and Tortorici, L. *Active faulting in the Calabrian arc and eastern Sicily*. J. Geodyn. **29**, 407-424 (2000).

(9) Billi, A., Barberi, G., Faccenna, C., Neri, G., Pepe, F. and Sulli A. *Tectonics and seismicity of the Tindari Fault System, southern Italy: crustal deformations at the transition between ongoing contractional and extensional domains located above the edge of a subducting slab*. Tectonics **25**, TC2006 (2006).

(10) Catalano, S. De Guidi, G. Monaco, C. Tortorici, G. and Tortorici, L. *Active faulting and seismicity along the Siculo–Calabrian Rift Zone (Southern Italy)*. Tectonophysics **453,** 177-192 (2008).

(11) Barreca, G., Bruno, V., Cultrera, F., Mattia, M., Monaco,C. and Scarfì, L. *New insights in the geodynamics of the Lipari–Vulcano area (Aeolian Archipelago, southern Italy) from geological, geodetic and seismological data.* J. Geodyn. **82**, 150-167 (2014).

(12) Barreca, G., Scarfì, L., Gross, F., Monaco, C. and De Guidi, G. *Fault pattern and seismotectonic potential at the south-western edge of the Ionian Subduction System (southern Italy): New field and geophysical constraints*. Tectonophysics **761,** 31-45 (2019).

(13) Orecchio, B., Presti, D., Totaro, C. and Neri, G. *What earthquakes say concerning residual subduction and STEP dynamics in the Calabrian Arc region, south Italy*. Geophys. J. Int. **199,** 1929-1942 (2014).

(14) Cultrera, F., Barreca, G., Burrato, P., Ferranti, L., Monaco, C., Passaro, S., Pepe, F. and Scarfì, L. *Active faulting and continental slope instability in the Gulf of Patti (Tyrrhenian side of NE Sicily, Italy): a field, marine and seismological joint analysis*. Nat.Hazards **86,** 253- 272 (2017).

(15) Cirrincione, R., Fazio, E., Fiannacca, P., Ortolano, G., Pezzino, A. and Punturo, R. *The Calabria-Peloritani Orogen, a composite terrane in Central Mediterranean; its overall architecture and geodynamic significance for a pre-Alpine scenario around the Tethyan basin*. Period. Mineral.**84,** 701-749 (2015).

(16) Ogniben, L. *Nota illustrativa dello schema geologico della Sicilia nord-orientale*. Riv. Min. Sic.**11,** 183-212 (1960).

(17) Catalano, S., Cirrincione, R., Mazzoleni, P., Pavano, F., Pezzino, A., Romagnoli, G. and Tortorici, G. *The effects of a Meso-Alpine collision event on the tectono-metamorphic evolution of the Peloritani mountain belt (eastern Sicily, southern Italy)*. Geol. Mag. **155,** 422-437 (2017).

(18) Rottura, A., Bargossi, G. M., Caironi, V., Del Moro, A., Maccarrone, E., Macera, P., Paglionico, A., Petrini, R., Piccareta, G. and Poli, G. *Petrogenesis of contrasting Hercynian granitoids from the Calabrian Arc, Southern Italy*. Lithos **24,** 97-119 (1990).

(19) Lentini, F. and Vezzani, L. *Tentativo di elaborazione di uno schema strutturale della Sicilia orientale*. Mem. Soc. Geol. It. **19,** 495-500 (1978).

(20) Pezzino, A. *Confronti petrografici e strutturali tra i basamenti metamorfici delle unità inferiori dei Monti Peloritani (Sicilia)*. Period. Mineral. **1,** 35-50 (1982).

(21) Acquafredda, P., Lorenzoni, S. and Zanettin Lorenzoni, E. *Palaeozoic sequences and evolution of the Calabrian-Peloritan Arc (Southern Italy)*. Terra Nova **6,** 582-594 (1994).

(22) Ferla, P. *A model of continental crust evolution in the geological history of the Peloritani Mountains (Sicily)*. Mem. Soc. Geol. It. **55,** 87-93 (2000).

(23) Trombetta, A., Cirrincione, R., Corfu, F., Mazzoleni, P. and Pezzino, A. *Mid-Ordovician U-Pb ages of porphyroids in the Peloritan Mountains (NE Sicily): palaeogeographical implications for the evolution of the Alboran microplate*. J. Geol. Soc. **161,** 265-276 (2004).

(24) Catalano, S. and Cinque, A. *L'evoluzione neotettonica dei Peloritani settentrionali (Sicilia nord-orientale): il contributo di una analisi geomorfologica preliminare.* Studi Geologici Camerti Special Issue **1995/2,** 113-123 (1995).

(25) Lee, K. Y., Moon, S. H., Oh, Y. H., Ha, K. and Ko, K. S. *Determination of the radon emanation fraction from rocks by simple gamma-ray spectrometry*. J. Radioanal. Nucl. Chem. **316,** 1307-1312 (2018).

(26) Sabatino, G., Di Bella, M., Caridi, F., Italiano, F., Romano, D., Magazù, S., Gnisci, A., Faggio, G., Messina, G., Santangelo, S., Leonetti, F. and Tripodo, A. *Radiological assessment, mineralogy and geochemistry of the heavy-mineral placers from the Calabrian coast (South Italy)*.J. Inst.**14,** P05015 (2019).

(27) Sakoda, A., Ishimori, Y. and Yamaoka, K. *A comprehensive review of radon emanation measurements for mineral, rock, soil, mill tailing and fly ash*. Appl. Radiat. Isot. **69,** 1422-1435 (2011).

(28) Angle4 Software (https://www.angle4.com/).

(29) Caridi, C., D'Agostino, M., Marguccio, S., Belvedere, A., Belmusto, G., Marcianò, G., Sabatino, G. and Mottese, A. *Radioactivity, granulometric and elemental analysis of river sediments samples from the coast of Calabria, south of Italy*. Eur. Phys. **131**, 136 (2016).

(30) Council directive 2013/59/EURATOM. *Laying down basic safety standards for protection against the dangers arising from exposure to ionising radiation*, and repealing Directives 89/618/Euratom, 90/641/Euratom, 96/29/Euratom, 97/43/Euratom and 2003/122/Euratom (2013).

(31) EC. Radiation protection 112, *Radiological Protection Principles Concerning the Natural Radioactivity of Building Materials*. (1999).

(32) IAEA. *Measurement and calculation of radon releases from NORM residues.* Technical Reports Series n◦ 474 International Atomic Energy Agency Vienna (2013).

(33) Arabi, A. S., Funtua, I. I., Dewu, B. B and Muhammad, A. M. *Background Radiation and Radiological Hazard Associated with Local Building Materials around Zaria, Nigeria*. Radiochemistry **57**, 207-212 (2015).

(34) Arabi, A. S., Funtua, I. I., Dewu, B. B. M., Kwaya, M. Y., Kurowska, E. K., Muhammad, A. M. and Garba, M. L. *NORM, radon emanation kinetics and analysis of rocks-associated radiological hazards*. Environ. Earth Sci.**75**, 689 (2016).

(35) Durridge Company, *RAD 7, electronic radon detector user manual* (http://www.durridge.com).

(36) Petropolous, M. P., Anagnostakis M. J., and Simopoulos, S. E. *Building Materials Radon Exhalation rate: ERRICCA Intercomparison Exercise Results*. Sci. Total Environ. **272,** 109-118 (2001).

(37) Tuccimei, P., Moroni, M. and Norcia, D. *Simultaneous determination of ^{222}Rn and ^{220}Rn exhalation rates from building materials used in Central Italy with accumulation chambers and a continuous solid state alpha detector: Influence of particle size, humidity and precursors concentration*. Appl. Radiat. Isot. **64,** 254-263 (2006).

(38) Dentoni, V., Da Pelo, S., Aghdam, M. M., Randaccio, P., Loi, A., Careddu, N. and Bernardini, A. *Natural radioactivity and radon exhalation rate of Sardinian dimension stones*. Constr. Build. Mater. **247,** 118377 (2020).

(39) Stoulos, S., Manolopoulou, M. and Papastefanou, C. *Assessment of natural radiation exposure and radon exhalation from building materials in Greece*. J. Environ. Radioact. **69,** 225-240 (2003).

(40) Ujic, P., Celikovic, I., Kandic, A., Vukanac, I., Durasevic, M., Dragosavac, D. and Zunic, Z. *Internal exposure from building materials exhaling ^{222}Rn and ^{220}Rn as compared to external exposure due to their natural radioactivity content.* App. Radiat. Isot. **68**, 201-206 (2010).

(41) Italian Legislation, D. Lgs. 230/1995.

(42) Bikit, I., Mrda, D., Grujic, S. and Kozmidic-Luburic, U. *Granulation effects on the radon emanation rate*. Radiat. Prot. Dosim. **145,** 184-188 (2011).

(43) Zhang, W., Zhang, Y. and Sun, Q. *Analyses of Influencing Factors for Radon Emanation and Exhalation in Soil*. Water Air Soil Pollut. **230,** 16 (2019).

(44) Sato, J. and Nakamura, T. *Leaching of radon from weathered granite into water.* Radioisotopes **42,** 667-675 (1993).

(45) Sakoda, A., Hanamoto, K., Ishinmori, Y., Nagamatsu, T. and Yamaoka, T. K. *Radioactivity and radon emanation fraction of the granites sampled at Misasa and Badgastein*. Appl. Radiat. Isot. **66,** 648-652 (2008).

(46) Barretto, P.M. *Emanation Characteristics of Terrestrial and Lunar Materials and the ^{222}Rn Loss Effect on the U–Pb System Discordance*. Ph. D thesis Rice University (1973).

(47) Giammanco, S., Palano, M., Scaltrito, A., Scarfì, L. and Sortino, F. *Possible role of fluid overpressure in the generation of earthquake swarms in active tectonic areas: The case of the Peloritani Mts. (Sicily, Italy).* J. Volcanol. Geother. Res. **178,** 795-806 (2008).

(48) El Afifi, E. M, Hilal, M. A., Khalifa, S. M. and Aly, H. F. *Evaluation of U, Th,K and emanated radon in some NORM and TENORM samples.* Radiat. Meas. **41**, 627-633 (2006).

(49) Misdaq, M. A. and Amghar, A. *Radon and thoron emanation from various marble materials: impact on the workers*. Radiat. Meas. **39,** 421-430 (2005).

(50) Akerblom, G. *Ground radon. Monitoring procedures in Sweden.* "JAG" Disc. Meeting on Radon Workshop, Geology, Environment, Technology, Royal Astronomical Society London (1993).

(51) Kumar, A., Chauhan, R. P., Joshi, M. and Sahoo, B. K. *Modeling of indoor radon concentration from radon exhalation rates of building materials and validation through measurements*. J. Environ. Radioact.**127**, 50-55 (2014).

(52) Hassan, N. M., Ishikawa, T., Hosoda, M., Iwaoka, K., Sorimachi, A., Sahoo, S. K., Janik, M., Kranrod, C., Yonehara, H., Fukushi, M. and Tokonami, S. *The effect of water content on the radon emanation coefficient for some building materials used in Japan.* Radiat. Meas. **46,** 232-237 (2011).

(53) Pereira, D., Neves, L., Pereira, A., Peinado, M., Blanco, J. A. and Tejado, J. J. *A radiological study of some ornamental stones: bluish granites from Extremadura (Spain).* Nat. Hazards Earth Sys. Sci. **12,** 395-401 (2012).

(54) UNSCEAR. *Report to the general assembly of the United Nations with scientific annexes*. United Nations New York (1993).

(55) Rovida, A., Locati, M., Camassi, R., Lolli,B. and Gasperini,P. *CPTI15, the 2015 version of the Parametric Catalogue of Italian Earthquakes.* Eds. INGV (2016).

(56) Irwin,W. P. and Barnes, I. *Tectonic relation of carbon dioxide discharges and earthquakes*. J. Geophys. Res .**85,** 3115-3121 (1980).

(57) Baubron, J. C., Rigo, A. and Toutain, J. P. *Soil gas profiles as a tool to characterize active tectonic areas: the Jaut Pass example (Pyrenees, France)*. Earth Planet. Sci. Lett. **196,** 69-81 (2002).

(58) Sciarra, A., Fascetti, A., Moretti, A., Cantucci, B., Pizzino, L., Lombardi, S. and Guerra, I. *Geochemical and radiometric profiles through an active fault in the Sila Massif (Calabria, Italy)*. J. Geochem. Explor. **148,** 128-137 (2015)

(59) Sciarra, A., Mazzini, A., Inguaggiato, S., Vita, F., Lupi, M. and Hadi, S. *Radon and carbon gas anomalies along the Watukosek Fault System and Lusi mud eruption, Indonesia*. Mar. Petrol. Geol. **90,** 77-90 (2018).

(60) Claesson, L., Skelton, A., Graham, C., Dietl, C., Morth, C. M., Torssander, P. and Kockum, I. *Hydrogeochemical changes before and after a major earthquake*. Geology **32,** 641-644 (2004).

(61) Yuce, G., Italiano, F., D'Alessandro, W., Yalcin, T. H., Yasin, D. U., Gulbay, A. H., Ozyurt, N. N., Rojay, B., Karabacak, V., Bellomo, S., Brusca, L., Yang, T., Fu, C. C., Lai, C. W., Ozacarand, A. and Walia, V. *Origin and interactions of fluids circulating over the Amik Basin (Hatay-Turkey) and relationships with the hydrologic, geologic and tectonic settings*. Chem. Geol. **388,** 23-39 (2014).

685
686
687
688

Tables

Table 1. Information, location and coordinates (UTM WGS84 zone 33S reference system) of the collected samples.

Sample ID	Type of rock	Tectonic Unit	Locality	North	East
ASP1	Late Variscan monzogranite	Aspromonte	Tono	4237468	549973
ASP2	Orthogneiss	Aspromonte	Marmara	4235290	541451
ASP3	Paragneiss	Aspromonte	Dinnammare	4223617	540613
ASP4	Amphibolite gneiss	Aspromonte	Dinnammare	4223594	540971
ASP5	Marble	Aspromonte	Tindari	4220994	504626
MAN1	Phyllite	Mandanici	Percia Rovetti	4211439	516590
SMU1	Metapelite	St. Marco d'Alunzio	Frascianida	4207313	516633
LTU1	Metapelite	Longi-Taormina	P.lla Pandolfo	4191929	524118
LTU2	Felsic porphyroid	Longi-Taormina	Castelmola	4190603	524346
LTU3	Intermediate meta-volcanite	Longi-Taormina	Castelmola	4190149	524643

691
692
693
694
695
696

Table 2. Activity concentration of ^{226}Ra, ^{232}Th and ^{40}K detected in the samples coming from the metamorphic basement of the Peloritani Belt, along with the calculated values of absorbed dose rate, annual effective dose outdoor and gamma index.

Sample ID	^{226}Ra (Bq kg^{-1})	^{232}Th (Bq kg^{-1})	^{40}K (Bq kg^{-1})	Adsorbed dose rate, D (nGy h^{-1})	Annual effective dose outdoor, $AEDE_{outdoor}$ (mSv y^{-1})	Gamma index, I
ASP1	18 ± 4	31 ± 9	1220 ± 176	78	0.096	0.62
ASP2	45 ± 6	77 ± 14	1345 ± 190	123	0.152	0.98
ASP3	40 ± 7	68 ± 17	1009 ± 163	102	0.125	0.81
ASP4	27 ± 5	15 ± 2	167 ± 84	28	0.035	0.22
ASP5	17 ± 4	14 ± 3	1060 ± 165	61	0.074	0.48
MAN1	40 ± 6	64 ± 15	1063 ± 168	101	0.124	0.81
SMU1	25 ± 4	36 ± 9	595 ± 100	58	0.071	0.46
LTU1	34 ± 6	39 ± 11	674 ± 127	67	0.083	0.53

LTU2	48 ± 7	47 ± 12	1760 ± 242	123	0.152	0.98
LTU3	56 ± 8	62 ± 14	785 ± 135	96	0.118	0.76

Table 3. Emanation coefficients and surface exhalation rates for the metamorphic samples resulting from the radon emanation experiment. The potential indoor radon activity concentration and the annual effective dose were also estimated.

Sample ID	**Emanation coefficient, ε (%)**	**Surface exhalation rate, E_S (Bq m^{-2} h^{-1})**	**Mass exhalation rate, E_M (mBq kg^{-1} h^{-1})**	**Indoor ^{222}Rn activity concetration, $Ci_{Rn(bm)}$ (Bq m^{-3})**	**Annual effective dose indoor, H (μSv y^{-1})**
ASP1	2.44 ± 0.9	0.30 ± 0.05	6.38 ± 1.10	0.77	19
ASP2	8.27 ± 1.6	2.75 ± 0.17	54.02 ± 3.26	6.99	176
ASP3	2.30 ± 0.7	0.63 ± 0.08	13.33 ± 1.70	1.60	40
ASP4	0.63 ± 0.3	0.12 ± 0.03	2.47 ± 0.69	0.30	8
ASP5	5.99 ± 1.9	0.82 ± 0.09	14.80 ± 1.63	2.08	53
MAN1	5.81 ± 1.3	1.56 ± 0.12	33.73 ± 2.69	3.95	100
SMU1	2.80 ± 0.8	0.50 ± 0.07	10.15 ± 1.45	1.27	32
LTU1	2.51 ± 0.8	0.62 ± 0.08	12.39 ± 1.62	1.57	39
LTU2	3.72 ± 1.1	1.27 ± 0.19	25.91 ± 3.78	3.22	81
LTU3	1.68 ± 0.4	0.72 ± 0.09	13.69 ± 1.62	1.83	46

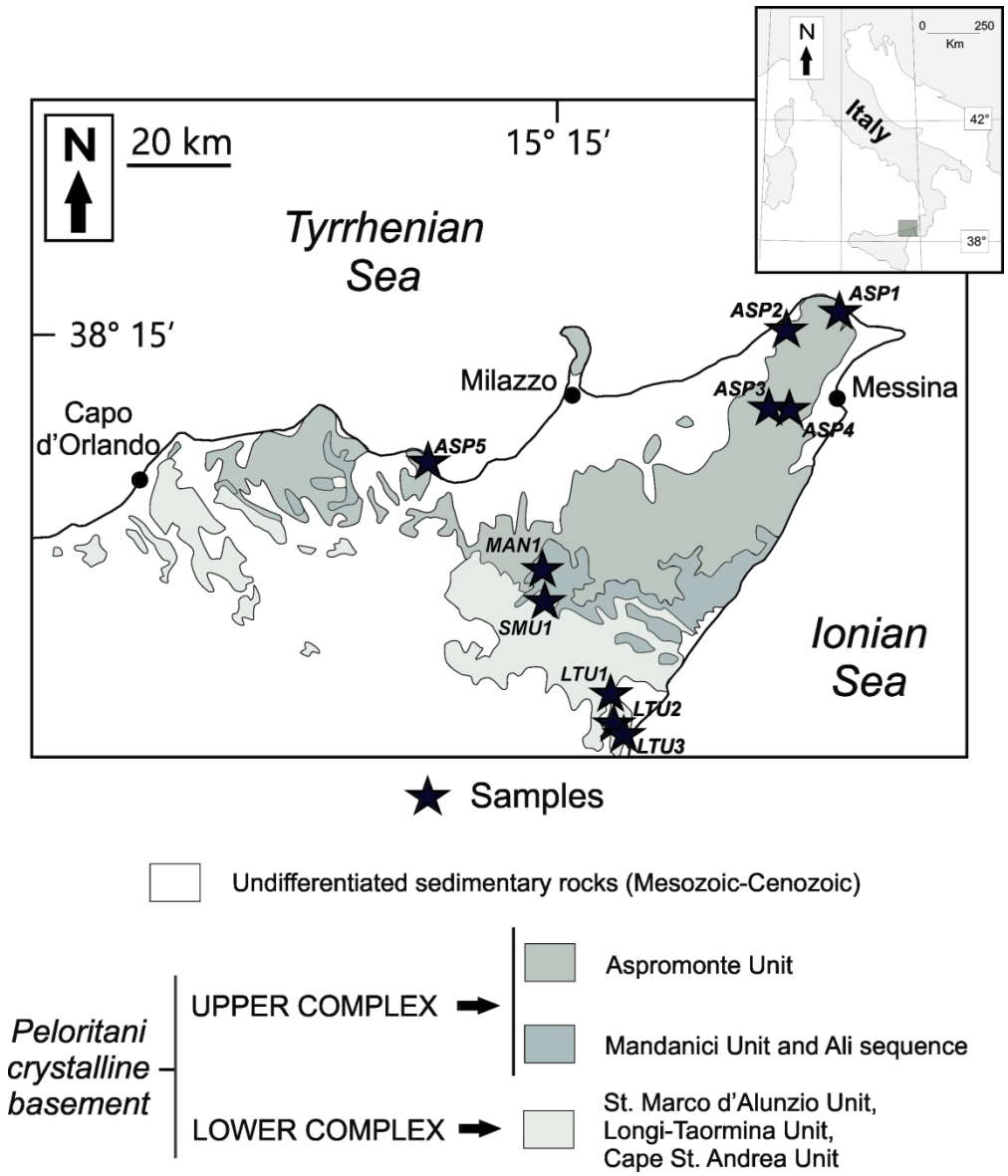

Figure 1. Geological sketch map of the Peloritani Belt (modified from Cirrincione et al.(15)); black stars: location of the collected samples.

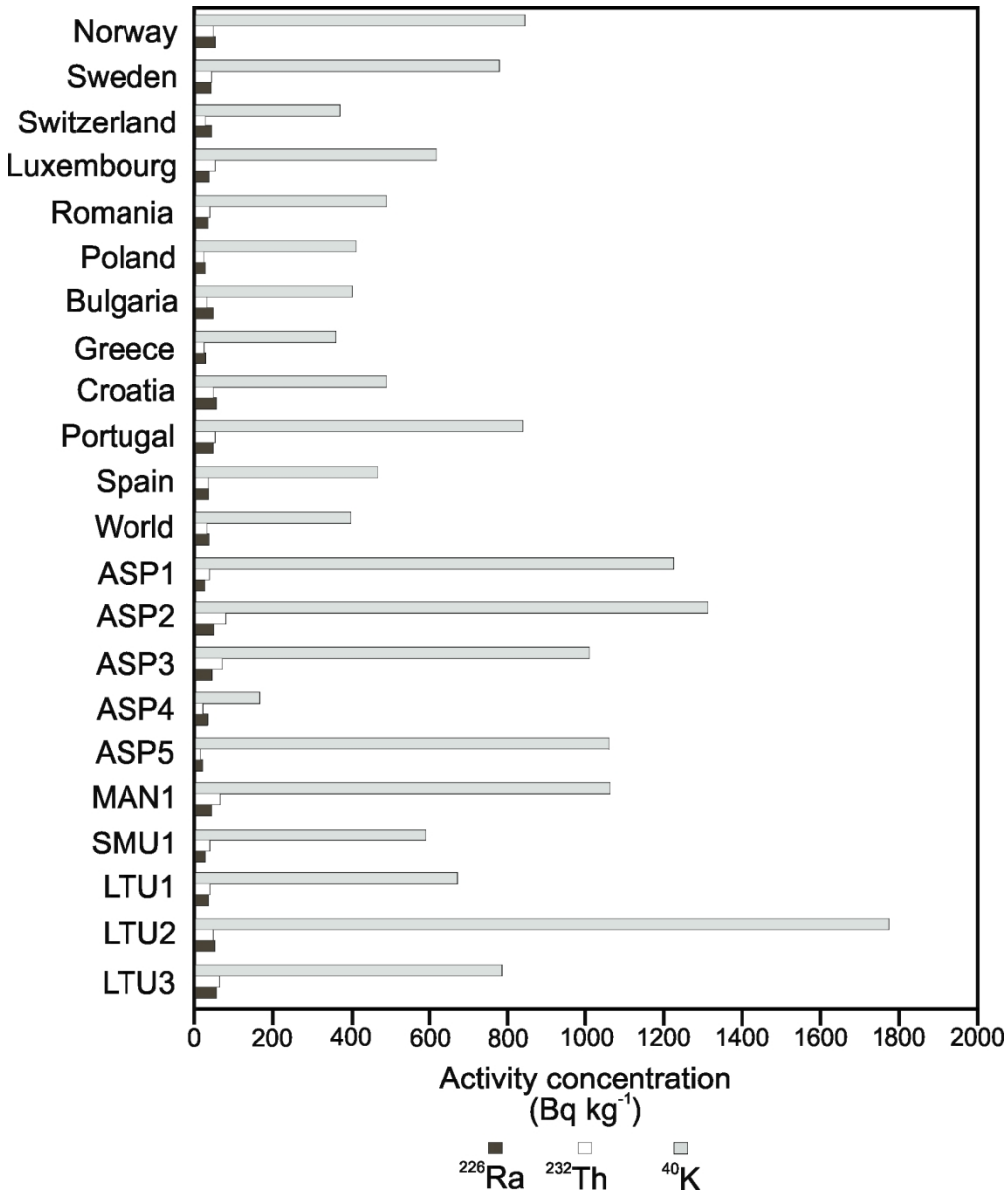

Figure 2. Activity concentrations of 226Ra, 232Th and 40K in the analysed samples compared with those of other European countries and with the worldwide average(1).